齊魯工業大學（山东省科学院）
QILU UNIVERSITY OF TECHNOLOGY SHANDONG ACADEMY OF SCIENCES

本科毕业论文

W-doped $MoTe_2$ modified separator and applications of lithium-sulfur battery

学院名称 化学与化工学院

专业班级 应化（国际班）19-1

学生姓名 张悦奇

学　　号 201996010111

导师姓名 顾少楠

2023 年 05 月 10 日

W-doped $MoTe_2$ modified separator and applications of lithium-sulfur battery

W 掺杂 $MoTe_2$ 改性隔膜及锂硫电池应用

学 院 名 称 化学与化工学院

专 业 班 级 应化（国际班）19-1

学 生 姓 名 张悦奇

学 号 201996010111

导 师 姓 名 顾少楠

专业技术职务 副教授

齐鲁工业大学本科毕业设计（论文）

原创性声明

本人郑重声明：所呈交的毕业设计（论文），是本人在指导教师的指导下独立研究、撰写的成果。设计（论文）中引用他人的文献、数据、图件、资料，均已在设计（论文）中加以说明，除此之外，本设计（论文）不含任何其他个人或集体已经发表或撰写的成果作品。对本文研究做出重要贡献的个人和集体，均已在文中作了明确说明并表示了谢意。本声明的法律结果由本人承担。

毕业设计（论文）作者签名：张悦奇

2023 年 05 月 10 日

齐鲁工业大学关于毕业设计（论文）

使用授权的说明

本毕业设计（论文）作者完全了解学校有关保留、使用毕业设计（论文）的规定，即：学校有权保留、送交设计（论文）的复印件，允许设计（论文）被查阅和借阅，学校可以公布设计（论文）的全部或部分内容，可以采用影印、扫描等复制手段保存本设计（论文）。

指导教师签名：　　毕业设计（论文）作者签名：张悦奇

2023 年　05　月　10　日　　2023　年　05　月　10　日

Contents

Abstract 1

摘　要 2

Chapter 1　Introduction 3

1.1 Background of lithium-sulfur batteries 3

1.2 Tangible limitations of lithium-sulfur batteries 4

1.3 Separators in lithium-sulfur batteries 6

1.4 Transition metal dichalcogenides and $MoTe_2$ 7

1.5 Tungsten (W) doping 9

1.6 Purpose and significance of this thesis 9

Chapter 2　Experimental 10

2.1 Chemicals and apparatus 10

2.2 Fabrication of W-doped $MoTe_2$/PP and $MoTe_2$/PP cells 11

2.2.1 Synthesis of pure $MoTe_2$ and W-doped $MoTe_2$ 11

2.2.2 Preparation of cathodes 12

2.2.3 Fabrication of cells 12

2.3 Characterization and electrochemical performance testing 13

2.3.1 Characterization 13

2.3.2 Electrochemical performance testing 13

Chapter 3　Results and Discussion 14

3.1 Characterization of materials 14

3.1.1 Scanning electron microscope（SEM） 14

3.1.2 Element mapping 15

3.1.3 X-ray diffraction (XRD) 16

3.1.4 X-ray photoelectron spectroscopy (XPS) 17

3.2 Performance research 18

3.2.1 Cyclic voltammetry (CV) curve 18

3.2.2 Impedance (EIS curve) 19

3.2.3 Galvanostatic charge and discharge curve 20
3.2.4 Long-term cycling curve 20
Chapter 4 Conclusion 22
Bibliography 23
Acknowledgements 27

Abstract

Energy demand rises consistently as a result of population growth, economic expansion, and lifestyle advancements. Concerns regarding environmental contamination brought on by the use of fossil fuels are growing more significant as energy consumption rises. Due to their higher theoretical energy density compared to other rechargeable systems, lithium-sulfur batteries have grown in popularity over the past two decades. However, numerous serious shortcomings with Li-S batteries, such as the dissolution and migration of polysulfides, the insulation, and the volume expansion during the cycling of sulfur, severely restrict their practical application. Numerous efforts have been made to resolve these issues, mainly including introducing conductive host for sulfur, catalyzing polysulfides fast conversion and protecting anode from lithium dendrite. Recently, separator functional modification has been the focus of significant research efforts aimed at restraining the polysulfides shuttling during discharge and charge.

In this thesis, the tungsten-doped molybdenum telluride (W-doped $MoTe_2$) was synthesized as a coating material for separators. Its catalytic effect on the performance for high lithium-sulfur batteries has been demonstrated by electro-chemical studies and analysis. Results indicate that cells using W-doped $MoTe_2$ modified separator presented almost no capacity decay at 4 C for 200 cycles, and had great capacity at 0.2 C.

Keywords: Li-S battery; modified separator; W doping; TMDs; catalyst design

摘 要

由于人口增长、经济发展和生活方式的进步，能源需求一直在上升。随着能源消耗的增加，人们对使用化石燃料所带来的环境污染的担忧也越来越严重。由于与其他可充电系统相比，锂硫电池具有更高的理论能量密度，在过去 20 年里，锂硫电池变得越来越受欢迎。然而，锂硫电池仍存在许多缺陷，如多硫化物的溶解和迁移、绝缘以及元素硫循环过程中的体积膨胀，而这些严重限制了其实际应用。为了解决这些问题，人们做出了许多努力，主要包括引入硫的导电载体，催化多硫化物的快速转化和保护阳极不受锂枝晶的影响。最近，隔膜的功能改性已经成为重要的研究重点，旨在抑制放电和充电过程中的多硫化物穿梭。

在本论文中，合成了钨掺杂的碲化钼（W 掺杂的 $MoTe_2$）作为隔膜的涂层材料进行改性。通过电化学研究和分析得到证明，它对锂硫电池性能具有催化作用。结果表明，W 掺杂的 $MoTe_2$ 改性隔膜电池在 4 C 的 200 次循环中几乎没有出现容量衰减，并且在 0.2 C 时下具有良好的容量。

关键词：锂硫电池　改性隔膜　钨掺杂　过渡金属硫化物　催化剂设计

Chapter 1 Introduction

1.1 Background of lithium-sulfur batteries

Nowadays, research on new energy technologies has been continuously boosted by the global warming and energy crisis. The need for better energy devices and more environmentally friendly energy sources accelerates the crucial research fields of energy generation and storage. As a result, electrochemical energy storage batteries are being developed and commercialized constantly, and the use of batteries will be essential for 2050 carbon neutrality.[1,2] With the high theoretical specific capacity (1,675 $mAh \cdot g^{-1}$ of S) and the high energy density (2,600 $Wh \cdot kg^{-1}$ of S), the increasing interest has been focused on lithium-sulfur (Li-S) batteries [3-5]

Typical advantages of Li-S battery include improved gravimetric energy density, a significantly reduced raw materials cost, improved safety characteristics and a reduced environmental burden associated with the cell materials. Li-S battery, whose gravimetric energy density can reach 400 $Wh \cdot kg^{-1}$ and beyond, enable vehicles to attain greater payload capacity, less weight, and longer mission endurance. Based on these, Li-S battery plays an imperative role in both the current and future vehicle applications such as large commercial vehicles (e.g., trucks and buses), high-altitude pseudosatellites (HAPS), electric vertical take-off and landing (eVTOL) and high-altitude long endurance (HALE).[6]

According to cell voltage, theoretical capacity, and theoretical specific energy, intriguing rechargeable battery systems are compared in Figure 1.[7] The highest possible theoretical energy densities are provided by metal-air or metal oxygen batteries including Li-air, Al-air, Mg-air and Li-air batteries. However, the high level of environmental sensitivity of the electrodes utilized in these batteries is a large obstacle to the real applications. Also, the tremendous volume change of these electrodes, which is caused by relevant electrochemical reactions, cannot be neglected.[7-8] By the contrast, even though Li-S battery shows lower theoretical energy densities, the low price of

material, relatively better cycling stability, and more environmentally friendly feature enable it to be a good candidate of many sorts of batteries.[7]

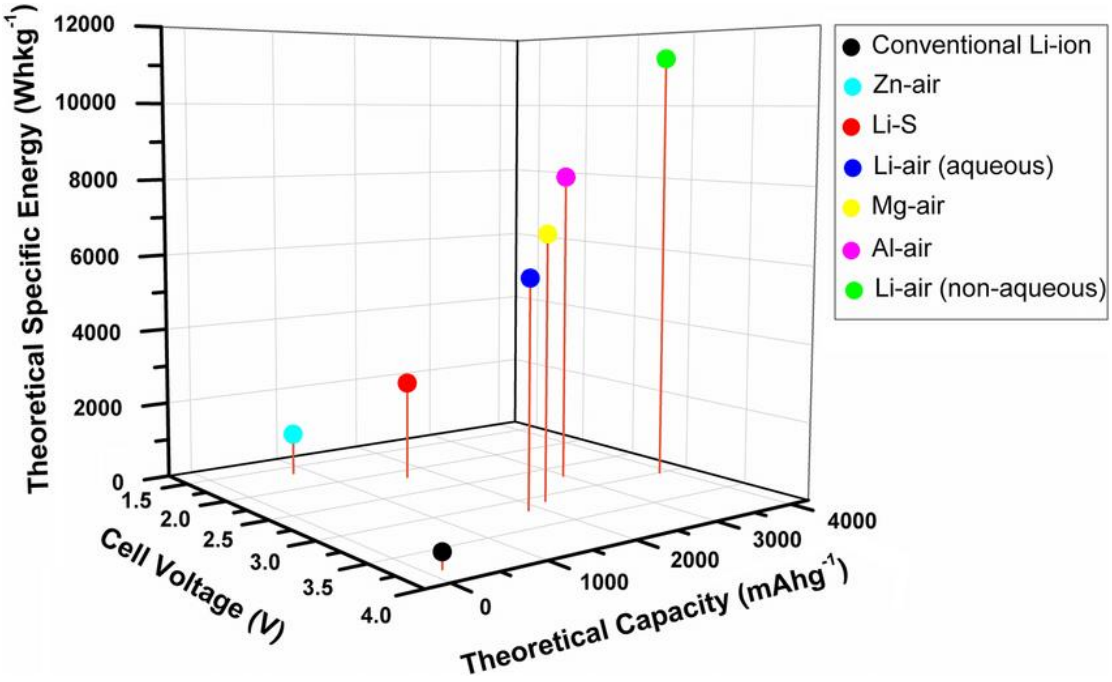

Figure 1. The theoretical capacity, cell voltage, and theoretical specific energy of several rechargeable battery systems[7]

1.2 Tangible limitations of lithium-sulfur batteries

Sufficient research has demonstrated that appealing advantages of Li-S battery give a substantial boost to the next-generation energy storage systems.[9] However, an abundance of issues are hindering the widespread use of Li-S batteries and related commercialization significantly.[10] Major issues with lithium sulfur systems include high electrical resistance, the shuttle effect, self-discharge, and volume expansion. These variables ultimately cause lithium-sulfur batteries to have a low Coulomb efficiency, rapid capacity degradation, and a short cycle life.

The structural instability can be caused by low electrical conductivity and huge volume expansion (up to 80%) of sulfur in cathode (Figure 2), and this structure fragmentation is able to cause conductive additive contact with sulfur to be lost, which leads to capacity decay.[11-12]

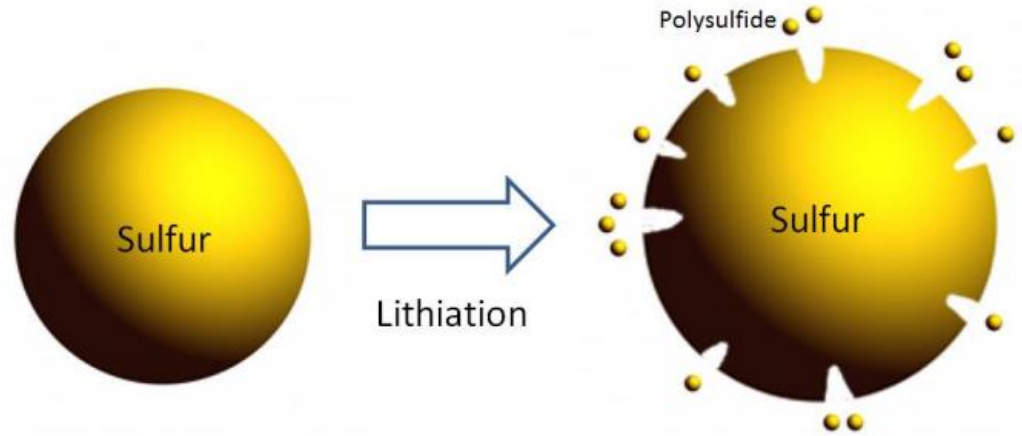

Figure 2. Volume expansion of lithium sulfur batteries[10]

In addition, lithium polysulfides (Li_2S_n, $4 \leq n \leq 8$), which are a kind of intermediate product of the cathode's reaction, act as a trigger for the irreversible loss of active substance due to the shuttle effect.[11] Elemental sulfur in solid state will dissolve into electrolyte after being discharged to high order polysulfide, where it will then react with the lithium anode to create low order polysulfide (Figure 3).[13] The physical condition of the electrolyte throughout the discharging process will go through a solid-liquid-solid transition process depending on how easily certain sulfur species can dissolve in it.[14]

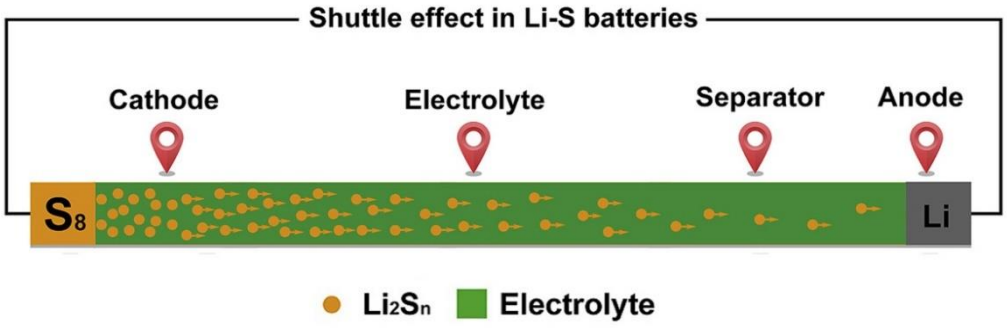

Figure 3. The shuttle effect in Li-S batteries[13]

As a result of this shuttle between the anode and cathode, solid Li_2S and Li_2S_2 are formed on the anode and the active material is lost, which give rise to low Coulombic efficiency, low sulfur cathode utilization, and significant cycle life degradation.[15]

The growth of dendrites occurs in the battery's internal structure (Figure 4), which take the blame for breakage of the barrier between the electrolyte and the lithium. The formation of lithium dendrite in anode will result in thermal failure and short circuit of the battery.[16]

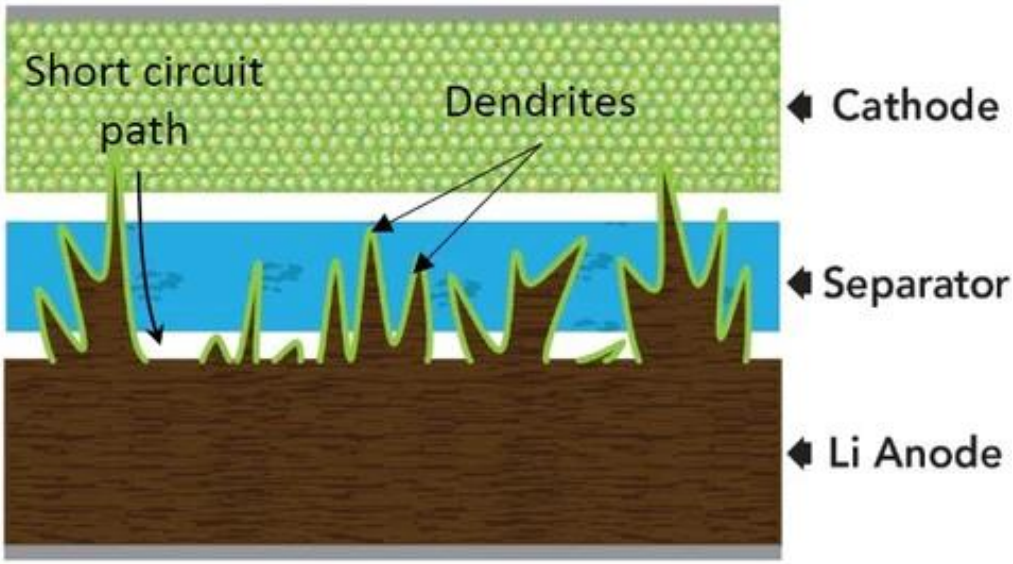

Figure 4. Dendrite growth in lithium battery leads to failure[16]

1.3 Separators in lithium-sulfur batteries

The separator, which is competent to guarantee the electrical isolation between the anode and cathode, is an essential part of the battery. Based on this main characteristic, the separator has the ability to move ions through its internal pores and protects the battery from electrical short circuits.[17] Nowadays, the increasing efforts have been put into a lot of modified separators for Li-S batteries.[18-20] Three types of commercial battery separators have been the most effective: the single-layer polyethylene separator (PE), the single-layer polypropylene separator (PP), and the three-layer PP/PE/PP composite separator. However, the shortcomings of these separators raise new problems. Due to the nature of lithium-ion batteries that require long-term cycling, these nonconductive separators, whose surface is greatly hydrophobic, cannot remain batteries' running effectively. [21]

The performance of Li-S batteries can be enhanced efficiently by adjusting the

physical and chemical features of the separator (Figure 5).[22] Physical adsorption, chemical adsorption, and electrostatic repulsion are some of the processes by which the modification materials significantly reduce the polysulfide shuttle effects. According to this, through introducing the modified coating to the separator or adding a special barrier layer between separator and cathode, the shuttle effect will be weakened in force. Additionally, due to the sufficient proximity of the modified separator and sulfur cathode, the separator can improve the utilization of sulfur, facilitate the redox reaction of adsorbed polysulfides, and even push the reactivation of the "dead sulfur".[21]

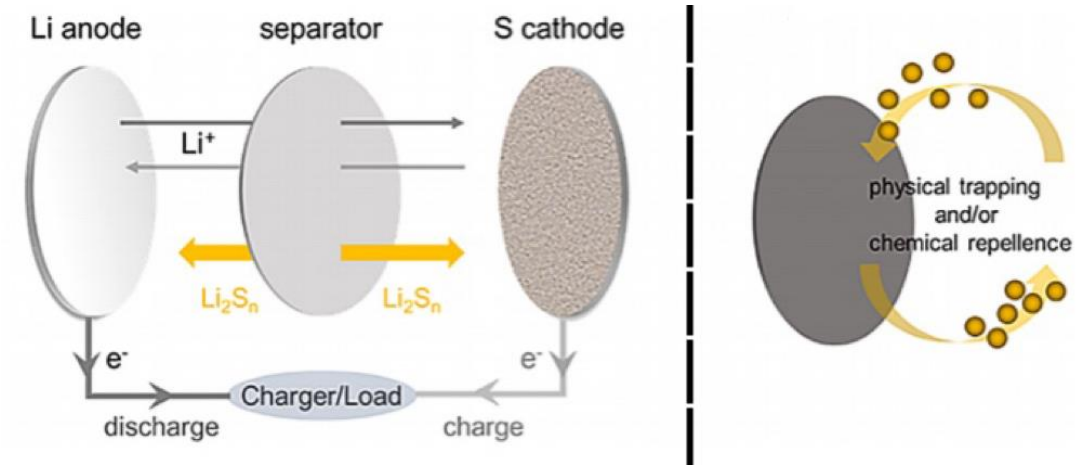

Figure 5. The shuttle effect of Li-S batteries (left) and a separator that acts as a barrier against polysulfide species (right)[22]

Coatings can be placed on porous polymer films to improve their related functions and performance.[23] The four main groups of these the separator coatings are polymer materials, carbon materials, inorganic compounds, MOFs, and COFs.[21]

1.4 Transition metal dichalcogenides and $MoTe_2$

2D materials are a diverse collection of substances with various chemical compositions and atomic structures. They exhibit a wide range of electronic properties, from insulators to superconductors.[24] Transition metal dichalcogenides (TMDs) are a

novel type of 2D nanosheet with the formula MX_2, where M is the transition metal and X is the chalcogen (Figure 6).[25]

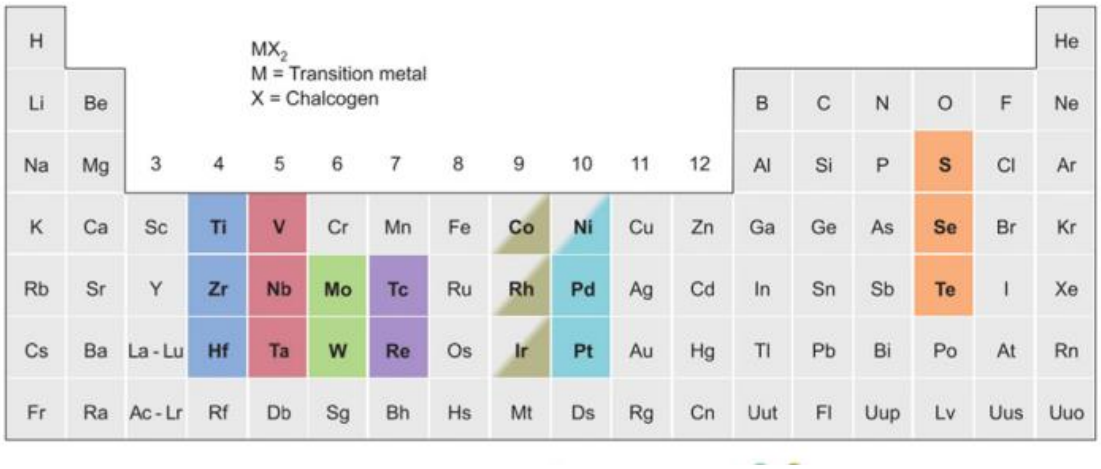

Figure 6. TMD materials with various element combinations indicated in a periodic table[24]

TMDs are a special class of 2D materials, which play diverse roles in polymorphs by virtue of main characteristics including superconductivity, semiconductivity, topological and metallic properties.[26] Hitherto, it has been demonstrated that 2D transition-metal dichalcogenides (TMDs, MOX_2 (X = S, Se)) are used as effective polar hosts and catalysts with dramatically increased performance in Li-S battery applications.[27, 28]

Recently, $MoTe_2$, as one example of TMDs, has aroused researchers' extensive attention in the field of Li-S batteries.[29] Panda et al.[30] have synthesized a 2D layered structured $MoTe_2$. Without any additional surface modifications or the addition of any conductive carbon coating, it was used directly as anode material. Moreover, depending on the prominent structural stability and considerable polar surface exposure, MoTe2 shows practical potential for absorbing the polysulfides and catalytic conversion, which support its use as a cathode host material.[31] However, on account of their high surface energy, pure $MoTe_2$ nanoparticles are prone to severe aggregation, which further reduces their surface area and active sites.[31-32] Therefore, Wei Z et al.[31] proposed anchoring MoTe2 to a carbon matrix with a large surface area and good conductivity,

which further inspired the $MoTe_2$ modified separator.

1.5 Tungsten (W) doping

Recent research has shown that doping with Tungsten (W) has exhibited its promising prospect in facilitating the electrochemical reactions. W doping strengthens the interaction between catalyst and reaction intermediates, so that the activity of catalyst can be increased.[33-35] It is also demonstrated that the enhancement of electrocatalytic water splitting activity can be observed via W doping in transition-metal phosphide, because it can influence the electronic structure.[36] Zhang L et al.[37] have shown that improvements in electrochemical conductivity and changes in the adsorption energy of hydrogen intermediates were both attributed to the addition of W.

1.6 Purpose and significance of this thesis

Li-S battery research has become increasingly in-depth in last decade due to the high theoretical specific capacity (1,675 $mAh \cdot g^{-1}$ of S) and the high energy density (2,600 $Wh \cdot kg^{-1}$ of S). $MoTe_2$ exhibits practical potential for catalytic conversion and polysulfide absorption due to the notable structural stability and significant polar surface exposure. The introduction of W promotes electrochemical reactions in Li-S batteries and may trigger synergistic effects with other catalysts. Therefore, the introduction of TMDs and heteroatom doping are also two promising strategies to improve the performance of batteries. Based on above theory, the significance of this work is to see whether the combination of W doping and $MoTe_2$ will help Li-S batteries perform better overall.

In this thesis, $MoTe_2$ and W-doped $MoTe_2$ coatings were synthesized successfully and applied to the separator of Li-S batteries. The comparison of two were conducted to observe how W doping improves the actual capacity and the cycling stability of Li-S batteries.

Chapter 2 Experimental

2.1 Chemicals and apparatus

The chemicals and instruments used in the experimental work of this thesis are listed in Table 1 and Table 2 by list of name, purity, and manufacturer.

Table.1 The list of chemicals followed by name, purity, manufacturer

Name	Purity	Manufacturer
Tellurium (Te)	AR	Shanghai Aladdin Biochemical Technology Co., Ltd.
Sodium borohydride ($NaBH_4$)	AR	Shanghai Aladdin Biochemical Technology Co., Ltd.
Sodium molybdate dihydrate ($Na_2MoO_4•2H_2O$)	AR	Shanghai Aladdin Biochemical Technology Co., Ltd.
Ammonium metatungstate ($(NH_4)_6H_2W_{12}O_{40}·XH_2O$)	AR	Shanghai Aladdin Biochemical Technology Co., Ltd.
Carbon nanotubes (CNT)	--	--
Sublimed Sulfur	AR	Damao Chemical Reagent Factory
Super P	--	--
polyvinylidene difluoride (PVDF)	--	Guangdong Canrd New Energy Technology Co.,Ltd.
N-Methylpyrrolidone (NMP)	AR	Shanghai Aladdin Biochemical Technology Co., Ltd.

Table.2 The list of apparatus followed by name and manufacturer

Name	Manufacturer
Electronic balance	Beijing Doris Science Instrument Co., Ltd.
Deionized water machine	Shanghai gaosen Instrument Co., Ltd.
Oil bath	--
Electric blast drying oven	Shanghai Yiheng Scientific Instrument Co.,Ltd.
Circulating water vacuum pump	Gongyi Yuhua Instrument Co., Ltd.
Planetary ball mill	--
Glovebox	--
LAND electrochemical station	--

2.2 Fabrication of W-doped $MoTe_2$/PP and $MoTe_2$/PP cells

2.2.1 Synthesis of pure $MoTe_2$ and W-doped $MoTe_2$

To synthesize W-doped $MoTe_2$, 12 mM (1.531 g) of tellurium metal powder (Te) was put into a beaker containing 60 ml of ultrapure water. The suspension was stirred vigorously and heated uniformly to 80℃ and 9 mM (0.34 g) $NaBH_4$ was added to the suspension in 3 portions and the temperature was maintained with continued stirring for about 3h. A large amount of Te power was dissolved to form a deep red NaHTe solution. 6 mM (1.452 g) of sodium molybdate dihydrate (Na_2MoO_4-$2H_20$) and 0.6 mM (0.89 g) of ammonium metatungstate ($(NH_4)_6H_2W_{12}O_{40}\cdot XH_2O$) were added sequentially in three portions, each at five-minute intervals.

The formed mixture was continued to stir for 30 min and then the mixture was transferred to a 100 ml PTFE reactor. It was heated to 200°C and maintained for 48 hours. The collected product was filtered, washed, and then dried at 80°C for several hours. Finally, to remove excess Te, the resulting powder was heated to 750°C (30 min ramp-up time) under Ar/H_2 flow gas (Ar = 30 scCm, H2 = 5 scCm) and maintained for 12 hours.

The synthesis of the pure $MoTe_2$ followed the same procedures as above, except that there was no ammonium metatungstate during the synthesis.

Both $MoTe_2$ and W-doped $MoTe_2$ slurry were configured to further make modified separators by virtue of coatings.

2.2.2 Preparation of cathodes

The composition of cathode slurry includes 80 wt% sulfur, 10 wt% Super P, and 10 wt% polyvinylidenefluoride (PVDF), which was used as a binder.

The preparation of cathode slurry started from sulfur filling. Initially, carbon nanotubes and sublimed sulfur were put into a mortar in a ratio of 30% and 70%, respectively, and grounded by hand for 30 minutes. After heating at 155℃ for 12 hours, the mixture, Super P and PVDF were further mixed in the ratio of 8:1:1 respectively, and then the ball-milling was conducted for 4 hours to acquire cathode slurry. Additionally, N-Methylpyrrolidone (NMP) was used to dissolve PVDF and dilute the slurry during the preparation.

The cathode slurry was coated on aluminum foil and then was vacuum dried sufficiently. The prepared cathodes were used to assemble cion cells afterwards.

2.2.3 Fabrication of cells

The coin cells were assembled in the laboratory glovebox with a Li chip as the anode, different prepared separators (PP, $MoTe_2$/PP, W-doped $MoTe_2$/PP), prepared cathodes containing sulfur, and 1.0 M LiTFSI in DOL/DME = 1:1 vol% with 1.0% LiNO3 as the electrolyte.

2.3 Characterization and electrochemical performance testing

2.3.1 Characterization

Element mapping was conducted to check whether W doping was successful. The composition and structure of the W-doped $MoTe_2$ were characterized by scanning electron microscope (SEM) and X-ray diffraction (XRD). X-ray photoelectron spectroscopy (XPS) was used to analyze the composition and chemical valence of the elements in the samples.

2.3.2 Electrochemical performance testing

The LAND battery test system was used to perform constant current charge/discharge test at room temperature, and the battery was tested for cycle life in the range of 1.7~2.8V. The cyclic voltammetric curve of the battery was recorded using an electrochemical workstation. Also, the impedance spectrum of the battery was tested.

Chapter 3 Results and Discussion

3.1 Characterization of materials

3.1.1 Scanning electron microscope（SEM）

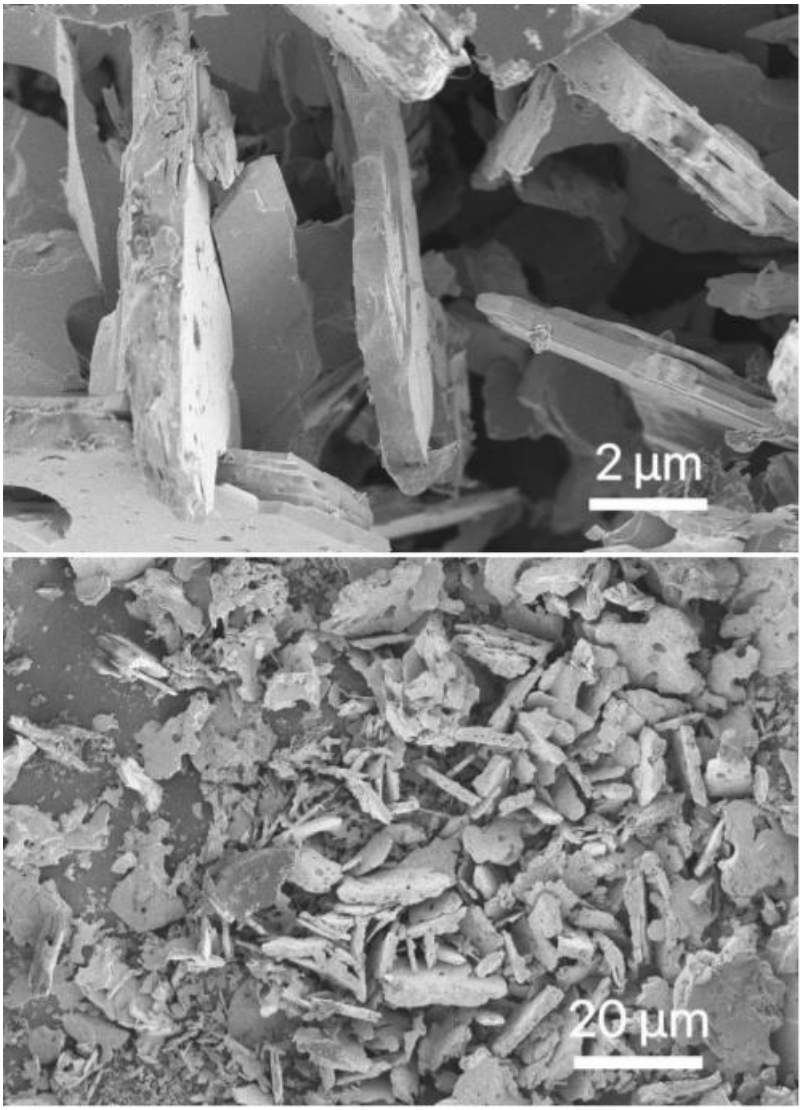

Figure 7. SEM images of W-doped $MoTe_2$ at different magnification

The SEM images of synthesized W-doped $MoTe_2$ are displayed in Figure 7. According to the SEM images, the synthesized product has irregular shape, and the stacking of two-dimensional sheet structure can be clearly observed, which are accord

with the two-dimensional crystal structure model of $MoTe_2$. The stacking of sheets provides the internal mutual support; thus, the stability of the material during the electrochemical process is ensured.

3.1.2 Element mapping

The element mapping of synthesized W-$MoTe_2$ was conducted to observe the element distribution (Figure 8).

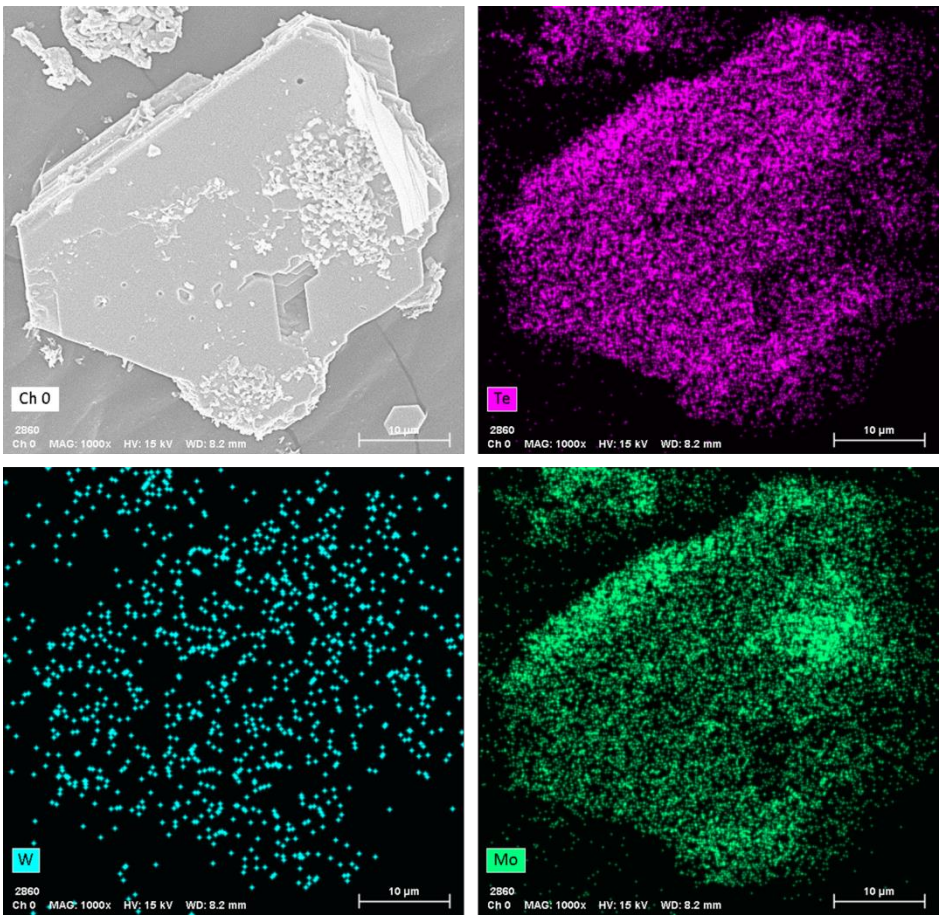

Figure 8. Element mapping of W-doped $MoTe_2$

As shown in Figure 8, the successfully doping was demonstrated by the uniform signal of W on $MoTe_2$. It is explicitly observed that the elements were distributed uniformly, which lays a solid foundation for the stable performance of batteries.

3.1.3 X-ray diffraction (XRD)

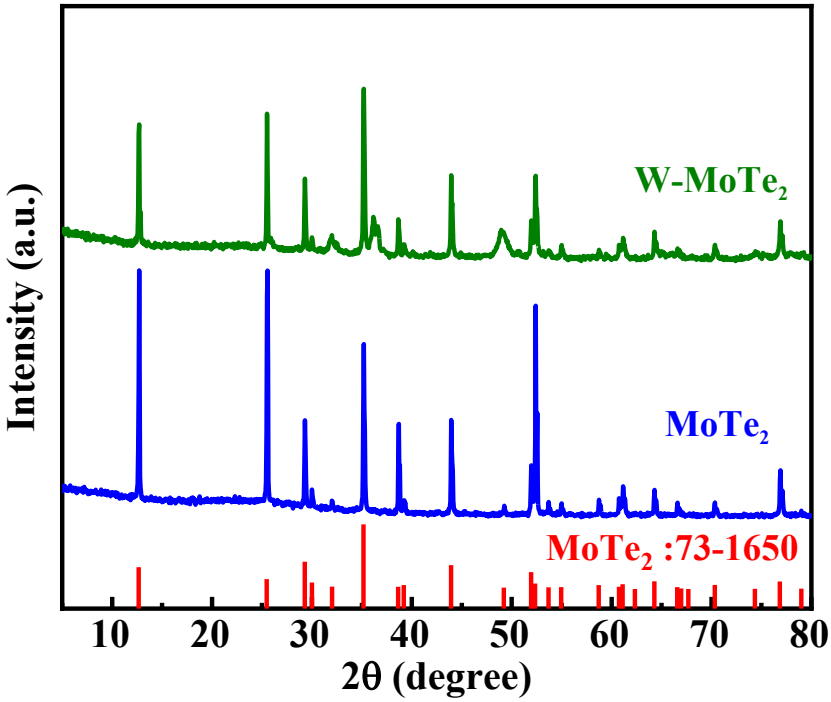

Figure 9. XRD image of W-doped $MoTe_2$ and $MoTe_2$

The results of XRD patterns are shown in Figure 9. The peaks of $MoTe_2$ and W-doped $MoTe_2$ highly correspond with JCPDS (No. 73-1650), indicating the no formation of other tungsten-based compounds after doping.

3.1.4 X-ray photoelectron spectroscopy (XPS)

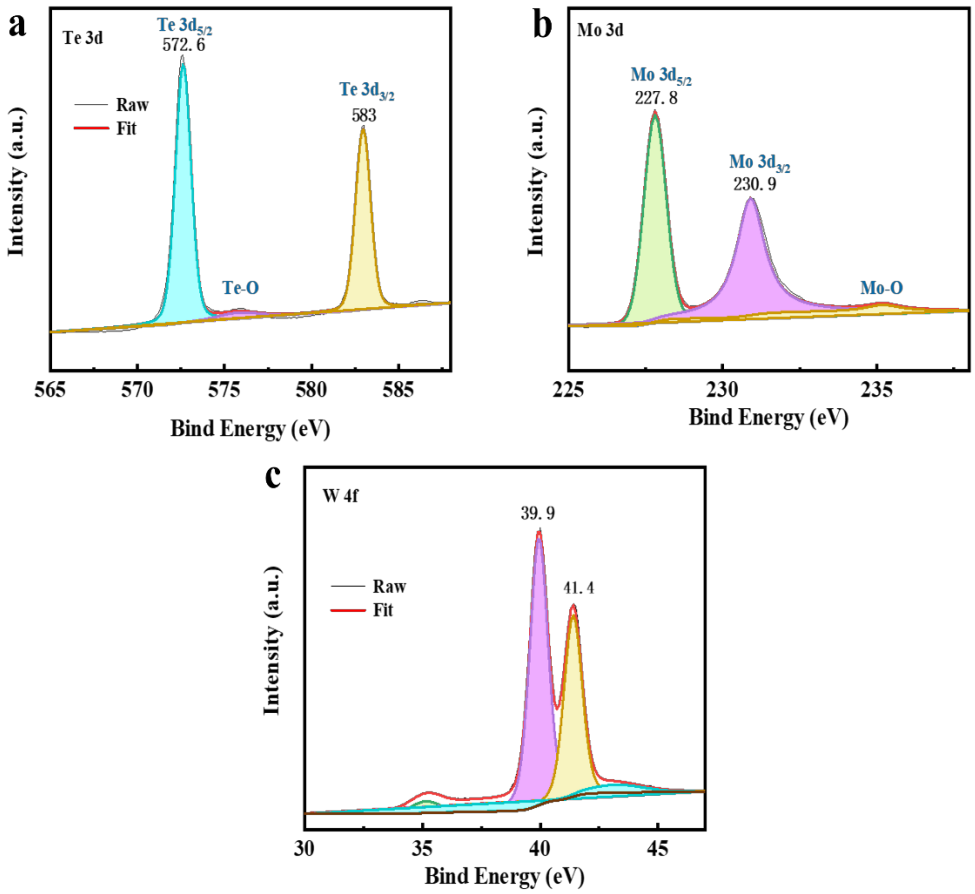

Figure 9. High-resolution XPS spectra of (a) Te 3d, (b) Mo 3d and (c)W 4f

Through utilizing the XPS test to analyze the synthesized W-doped $MoTe_2$, the elemental composition and valence of coatings for modified separator of Li-S batteries were confirmed precisely. As shown in Figure 9, Te, Mo and W are detected successfully. Additionally, the binding energy peaks of W-doped MoTe2 are acquired through Figure 9; The binding energy peaks of Te $3d_{5/2}$ and Te $3d_{3/2}$ are at 572.6 eV and 583 eV, respectively (Figure 9(a)). The binding energy peaks of Mo $3d_{5/2}$ and Mo $3d_{3/2}$ are at 227.8 eV and 230.9 eV, respectively (Figure 9(b)). The binding energy peaks of different W 4_f are at 39.9 eV and 41.4 eV, respectively (Figure 9(c)).

According to Figure 9 (a), an inconspicuous binding energy peak is noticed, which indicates the formation of chemical bond between tellurium in the material and oxygen,

and it is possibly caused by the reaction of tellurium with hydroxyl groups of water molecules in the air during the preservation of the material. Figure 9 (b) also shows the same phenomenon.

3.2 Performance research

3.2.1 Cyclic voltammetry (CV) curve

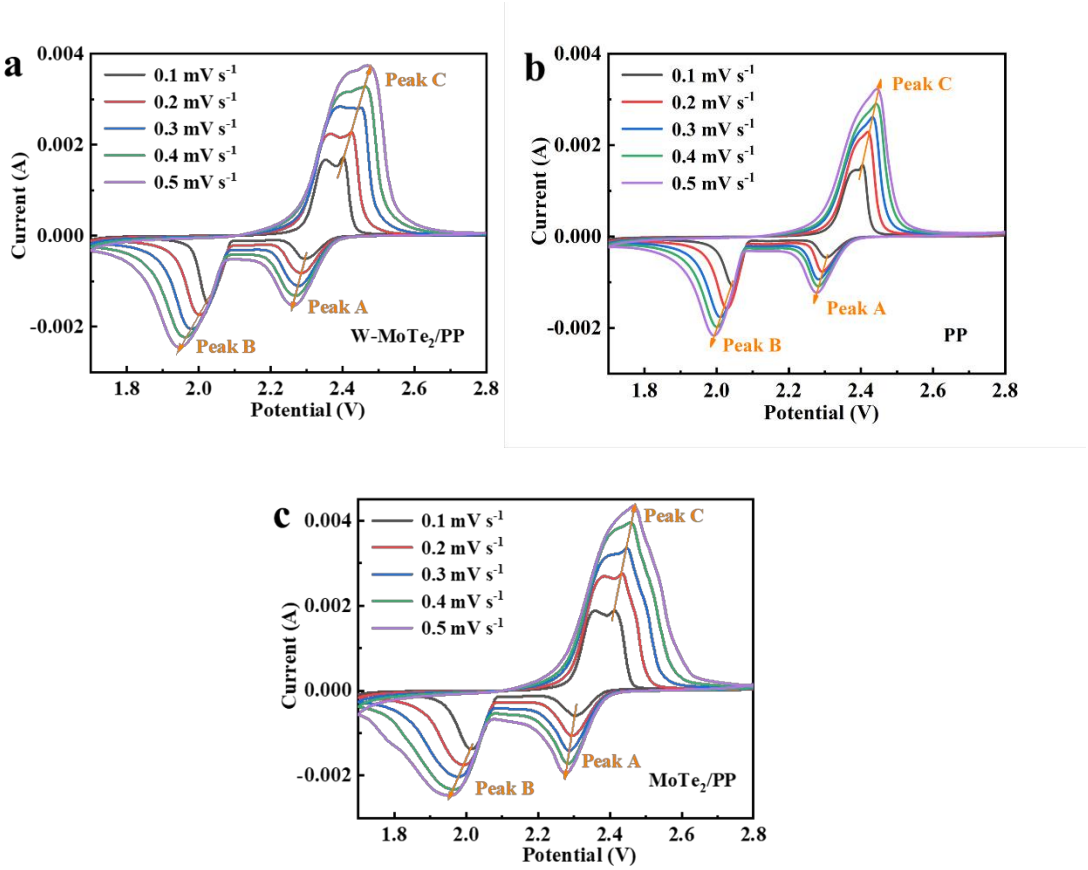

Figure 10. CV curves of (a) W-$MoTe_2$/PP, (b) PP and (c) $MoTe_2$/PP at different scanning rates

Figure 10 shows the CV curves of three different cells at five different scanning rates at 0.1, 0.2, 0.3, 0.4 and 0.5 mV s^{-1}, respectively. By analyzing the shape of curves, the reversibility of cells can be confirmed. There are two reduction peaks in discharge process, which correspond to the reduction of S_8 to long-chain polysulfides and the reduction of long-chain polysulfides to Li_2S. As shown in Figure 10, the slopes of the

fitted redox peak curves at different rates of both W-doped $MoTe_2$ and $MoTe_2$ modified separator cells are prominently higher than those of cells without the modified separators. Thus, the more satisfactory battery performance caused by increased kinetics can be demonstrated.

3.2.2 Impedance (EIS curve)

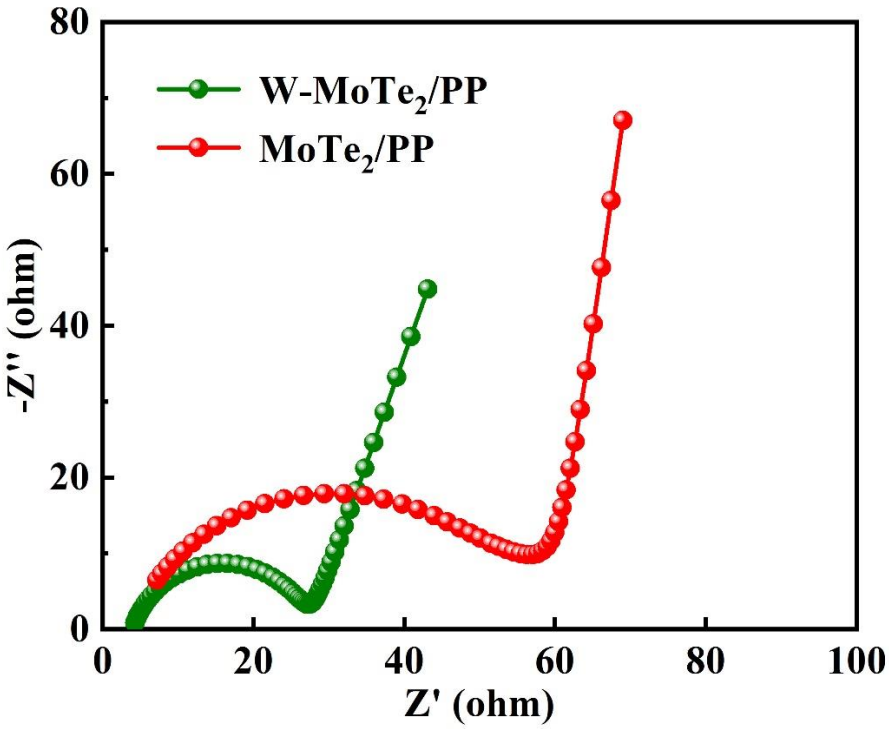

Figure 11. EIS curve of W-doped $MoTe_2$ and $MoTe_2$ modified separator cells

EIS test comparing the electrochemical impedance with W-doped $MoTe_2$/PP and $MoTe_2$/PP (Figure 11). The corresponding semicircle corresponds to the charge transfer impedance at the interface between the electrode and the electrolyte, and the diagonal part represents the Weber impedance. The use of W-doped $MoTe_2$ can act as an efficient chemical anchor catalyst to accelerate conversion kinetics and catalytic reactions of lithium polysulfides, and thus the redox reaction in Li-S batteries can be sped up. Consequently, from Figure 13, it is clearly observed that the impedance of W-doped

$MoTe_2$/PP is much smaller.

3.2.3 Galvanostatic charge and discharge curve

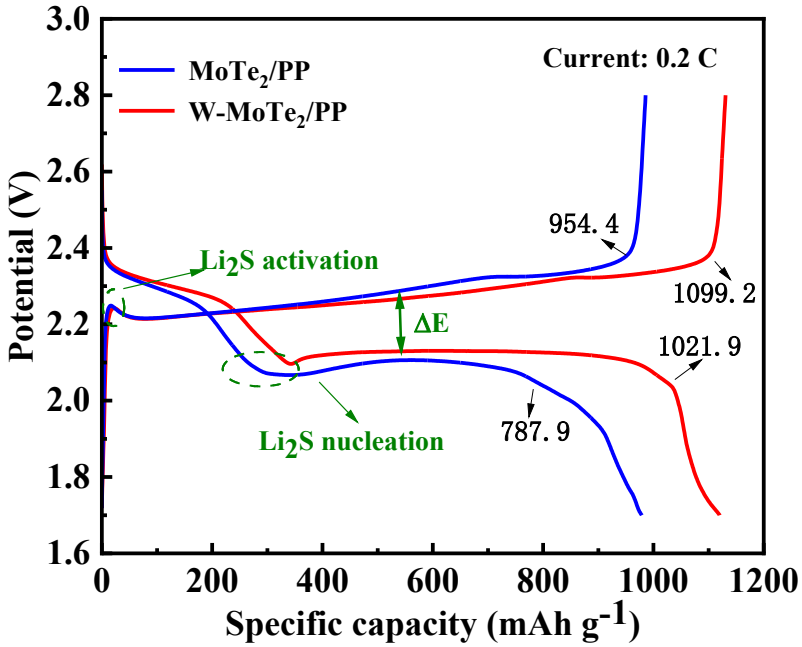

Figure 12. Galvanostatic charge and discharge curve of different cells at 0.2 C

As shown in Figure 12, the W-doped $MoTe_2$ modified separator cells' initial discharge plateau at 0.2 C is noticeably protracted, which led to a higher capacity of 1021.9 $mAh \cdot g^{-1}$ compared to $MoTe_2$ modified separator cells whose capacity is 787.9 $mAh \cdot g^{-1}$.The W-doped $MoTe_2$ modified separator cells possess the narrowest voltage gap (ΔE) between the oxidation and reduction plateaus, further indicating the use of W-doped $MoTe_2$ modified separator can tangibly enhance the connection across electrodes.[38]

3.2.4 Long-term cycling curve

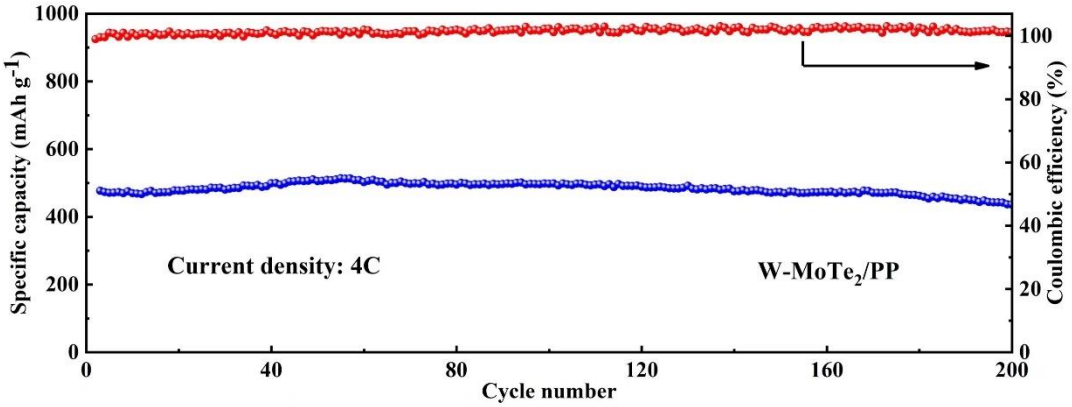

Figure 13. Long-term cycling performance at 4 C of cells using W-doped $MoTe_2$ modified separators for 200 cycles

Figure 13 indicates the long-term cycling performance at 4 C of W-doped $MoTe_2$ modified separator cells for 200 cycles. The initial charge specific capacity is about 500 $mAh \cdot g^{-1}$, and there is no significant capacity decay at 4 C for 200 cycles, indicating the sufficient cycling stability.

Chapter 4 Conclusion

In summary, the successful doping method was adopted to synthesize Tungsten-doped Molybdenum telluride (W-doped $MoTe_2$) by virtue of the reaction among tellurium (Te), sodium borohydride ($NaBH_4$), sodium molybdate dihydrate ($Na_2MoO_4•2H_2O$) and Ammonium metatungstate ($(NH_4)_6H_2W_{12}O_{40}·XH_2O$). Through material characterization, the successful synthesis of the material was determined, and the internal two-dimensional sheet structure was observed. By testing the performance of W-doped $MoTe_2$, $MoTe_2$ modified separator cells and cells without the modified separators, it was demonstrated that W-doped $MoTe_2$ modified separator can tangibly improve the performance of Li-S batteries in terms of the capacity, coulombic efficiency, connection across electrodes and impedance.

The apparent errors cannot be neglected in this work, and the reasons can be complicated. Specifically, to avoid errors as much as possible, the increasing number of experiments is needed. Moreover, the difficulties in this work mainly lied on the synthesis of the material and the doping method. The duration of the reaction, the adequacy of the materials used, and the choice of doping chemicals all may affect the performance of the synthesized material in the test.

Overall, the experiment went relatively smoothly, and results meet the satisfactory standard.

Bibliography

1. LIN J, ZHANG X, FAN E, et al.，. Carbon neutrality strategies for sustainable batteries: From structure, recycling, and properties to applications[J]. Energy & Environmental Science, 2023, 16(3): 745–791.
2. BARGHAMADI M, KAPOOR A, WEN C，. A review on Li-S Batteries as a high efficiency rechargeable lithium battery[J]. Journal of The Electrochemical Society,2013, 160(8).
3. HE J, MANTHIRAM A，. A review on the status and challenges of electrocatalysts in lithium-sulfur batteries[J]. Energy Storage Materials, 2019, 20: 55–70.
4. WANG P, XI B, HUANG M, et al.，. Emerging catalysts to promote kinetics of lithium–sulfur batteries[J]. Advanced Energy Materials, 2021, 11(7): 2002893.
5. ZHENG J, TIAN J, WU D, et al.，. Lewis acid–base interactions between polysulfides and metal organic framework in lithium sulfur batteries[J]. Nano Letters, 2014, 14(5): 2345–2352.
6. DÖRFLER S, WALUS S, LOCKE J, et al.，. Recent progress and emerging application areas for lithium–sulfur battery technology[J]. Energy Technology, 2020, 9(1):2000694.
7. Gupta A, Sivaram S. Separator membranes for lithium–sulfur batteries: Design principles, structure, and performance[J]. Energy Technology, 2019, 7(6): 1800819.
8. Bruce P G, Freunberger S A, Hardwick L J, et al. Li–O2 and Li–S batteries with high energy storage[J]. Nature Materials, 2011, 11(1): 19–29.
9. XU R, LU J, AMINE K，. Progress in mechanistic understanding and characterization techniques of Li-S Batteries[J]. Advanced Energy Materials, 2015, 5(16): 1500408.
10. WEI Z, REN Y, SOKOLOWSKI J, et al.，. Mechanistic understanding of the role separators playing in advanced lithium-sulfur batteries[J]. InfoMat, 2020, 2(3): 483–508.
11. MANTHIRAM A, FU Y, CHUNG S-H, et al.，. Rechargeable lithium–sulfur batteries[J]. Chemical Reviews, 2014, 114(23): 11751–11787.
12. Chen, Xi. Rational Design of Cathode Materials for High Performance Lithium-Sulfur Batteries[D]. Milwaukee: University of Wisconsin–Milwaukee, 2016
13. Ren W, Ma W, Zhang S, et al. Recent advances in shuttle effect inhibition for lithium sulfur batteries[J]. Energy Storage Materials, 2019, 23: 707–732.

14. MANTHIRAM A, FU Y, SU Y-S，. Challenges and prospects of lithium–sulfur batteries[J]. Accounts of Chemical Research, 2012, 46(5): 1125–1134.
15. Cheng X-B, Huang J-Q, Peng H-J, et al. Polysulfide Shuttle control: Towards a lithium-sulfur battery with superior capacity performance up to 1000 cycles by matching the sulfur/electrolyte loading[J]. Journal of Power Sources, 2014, 253: 263–268.\
16. Li W, Yao H, Yan K, et al. The synergetic effect of lithium polysulfide and lithium nitrate to prevent lithium dendrite growth[J]. Nature Communications, 2015, 6(1).
17. Arora P, Zhang Z. Battery separators[J]. Chemical Reviews, 2004, 104(10): 4419–4462.
18. Chen H, Xiao Y, Chen C, et al. Conductive MOF-modified separator for mitigating the shuttle effect of lithium–sulfur battery through a filtration method[J]. ACS Applied Materials & Interfaces, 2019, 11(12): 11459–11465.
19. Abbas S A, Kaisar N, Chen Y-T, et al. Modified separators with ultrathin graphite coating simultaneously mitigate the issues of metal dendrites and lithium polysulfides to provide stable lithium–sulfur batteries[J]. ACS Sustainable Chemistry & Engineering, 2019, 7(19): 16604–16611.
20. Moorthy B, Kwon S, Kim J-H, et al. Tin sulfide modified separator as an efficient polysulfide trapper for stable cycling performance in Li–S Batteries[J]. Nanoscale Horizons, 2019, 4(1): 214–222.
21. Li C, Liu R, Xiao Y, et al. Recent progress of separators in lithium-sulfur batteries[J]. Energy Storage Materials, 2021, 40: 439–460.
22. Xiang Y, Li J, Lei J, et al. Advanced separators for lithium-ion and lithium-sulfur batteries: A review of recent progress[J]. ChemSusChem, 2016, 9(21): 3023–3039.
23. Luo W, Cheng S, Wu M, et al. A review of advanced separators for rechargeable batteries[J]. Journal of Power Sources, 2021, 509: 230372.
24. Lin J, Zhou W. Defect in 2D materials beyond graphene[J]. Defects in Advanced Electronic Materials and Novel Low Dimensional Structures, 2018: 161–187.
25. Chen Y, Wang L, Shi J, et al. Two-dimensional non-carbonaceous materials-enabled efficient photothermal cancer therapy[J]. Nano Today, 2016, 11(3): 292–308.
26. PAUL S, TALUKDAR S, SINGH R S, et al.，. Topological Phase Transition in MoTe2: A

Review[J]. physica status solidi (RRL) – Rapid Research Letters, 2022: 2200420.

27. HE J, HARTMANN G, LEE M, et al.，. Freestanding 1T MOS2/graphene heterostructures as a highly efficient electrocatalyst for lithium polysulfides in Li–S Batteries[J]. Energy & Environmental Science, 2019, 12(1): 344–350.
28. YU B, CHEN Y, WANG Z, et al.，. 1T-MOS2 nanotubes wrapped with N-doped graphene as highly-efficient absorbent and electrocatalyst for Li–S Batteries[J]. Journal of Power Sources, 2020, 447: 227364.
29. Panda M R, Gangwar R, Muthuraj D, et al. High Performance Lithium-Ion Batteries Using Layered 2H-$MoTe_2$ as Anode[J]. Small, 2020, 16(38): 2002669.
30. Panda M R, Raj K A, Ghosh A, et al. Blocks of molybdenum ditelluride: A high rate anode for sodium-ion battery and full cell prototype study[J]. Nano Energy, 2019, 64: 103951.
31. Wei Z, Sarwar S, Azam S, et al. Ultrafast microwave synthesis of $MoTe_2$@graphene composites accelerating polysulfide conversion and promoting Li_2S nucleation for high-performance Li-S Batteries[J]. Journal of Colloid and Interface Science, 2023, 635: 391–405.
32. Cheng S, Yang L, Li J, et al. Large area, phase-controlled growth of few-layer, two-dimensional $MoTe_2$ and lateral 1T′–2H heterostructures by chemical vapor deposition[J]. CrystEngComm, 2017, 19(7): 1045–1051.
33. Yan J, Kong L, Ji Y, et al. Single atom tungsten doped ultrathin α-$Ni(OH)_2$ for enhanced electrocatalytic water oxidation[J]. Nature Communications, 2019, 10(1).
34. Lu S-S, Zhang L-M, Dong Y-W, et al. Tungsten-doped Ni–Co phosphides with multiple catalytic sites as efficient electrocatalysts for overall water splitting[J]. Journal of Materials Chemistry A, 2019, 7(28): 16859–16866.
35. Wang X, Chen Y, Yu B, et al. Hierarchically Porous W-Doped CoP Nanoflake Arrays as Highly Efficient and Stable Electrocatalyst for pH-Universal Hydrogen Evolution[J]. Small, 2019, 15(37): 1902613.
36. Ghosh S, Kadam S R, Kolatkar S L, et al. W Doping in $Ni_{12}P_5$ as a Platform to Enhance Overall Electrochemical Water Splitting[J]. ACS Applied Materials & Interfaces, 2021, 14(1): 581–589.
37. Zhang L, Liu P F, Li Y H, et al. Accelerating neutral hydrogen evolution with tungsten

modulated amorphous metal hydroxides[J]. ACS Catalysis, 2018, 8(6): 5200–5205.

38. GU S, XU S, SONG X, et al. Electrostatic Potential-Induced Co–N4 Active Centers in a 2D Conductive Metal–Organic Framework for High-Performance Lithium–Sulfur Batteries[J]. ACS Applied Materials & Interfaces, 2022, 14(45): 50815–50826.

Acknowledgements

As I come to the end of this journey, I am overwhelmed with a deep sense of emotion. The challenges and triumphs of this journey have molded me into the person I am today, and I am forever grateful for those who have supported me.

Thanks to my supervisor, Prof. Shaonan Gu, who has provided me with a wealth of academic guidance, both in your classes and throughout this graduation design. It is my great honor to be your student.

Thanks to my senior, Meng Guo, who has been always responsible and assisted me with a variety of issues in this thesis work.

Thanks to my referrers in Finland, Dr. Johannes Jermakka and Dr. Päivi Viitaharju, who enthusiastically helped me in master program applications. Your dedication to science will always inspire me in my future endeavours.

Thanks to my friends, Chengji Yang and Guoqiang Shi. Your company is a precious gift to my university life.

Thanks to Boman Li, who always listened and comforted me. It is my fortune to progress with you.

Thanks to my aunt, li Peng. You once said that family is always my strongest support, so I hope to be your support in the future, too.

Thanks to my parents, Ying Peng and Bingzheng Zhang, who always led and support me selflessly. I love you forever.

Thanks to myself. Thank you for your unwavering commitment to your dreams and your unyielding belief in yourself.